Preprints of the 21st IFAC World Congress (Virtual)
Berlin, Germany, July 12-17, 2020

On strongly unimodal third-order SISO linear systems with applications to pharmacokinetics

Steven R. Weller, * **Jennifer H. Martin** **

* *School of Electrical Engineering and Computing University of Newcastle, Callaghan, NSW 2308, Australia e-mail: steven.weller@newcastle.edu.au*
** *Centre for Human Drug Research, School of Medicine and Public Health, University of Newcastle, Hunter Medical Research Institute, NSW 2305, Australia e-mail: jenniferh.martin@newcastle.edu.au*

Abstract:
This paper addresses the problem of characterizing external positivity (equivalently, non-negative impulse response) of third-order single-input, single-output (SISO) linear systems. We show how an exact, geometric solution to this problem follows by first identifying an equivalence between the impulse response of an externally positive system on the one hand, and the probability density function of a non-negative random variable on the other, then drawing on the characterization of matrix exponential distributions, defined as probability distributions for which the Laplace transform is a rational function. The results are then extended to the characterization of strongly unimodal systems, defined as systems in which input signals with a time-derivative that has at most one sign variation (namely, are pulse-like) are mapped to output signals with the same property. The results are applied to a third-order compartmental system arising in pharmacokinetics, in which the properties of non-negativity of the impulse response and the preservation of unimodality from drug adminstration (input) to compartmental drug concentration (output) are of clinical relevance.

Keywords: time-invariant systems, externally positive systems, non-negative impulse response, compartmental modelling, strong unimodality, pharmacokinetics and drug delivery

1. INTRODUCTION

Many systems are described by physical quantities which are intrinsically constrained to be non-negative, such as chemical concentrations, population levels and queue lengths. Systems subject to these constraints—known as *positive systems*—are abundant in practical applications spanning biology, ecology, pharmacology, biochemistry, network flows, epidemiology and economics, and are of longstanding system theoretical interest.

For linear state-space models, a distinction needs to be drawn between *internal positivity* (or simply "positivity") and *external positivity*, also known as input–output positivity; see Farina and Rinaldi (2000). Continuous-time (internally) positive, linear time-invariant (LTI) systems in state-space form are readily characterized; namely A is required to be Metzler, while B, C and D necessarily have non-negative entries; see Farina and Rinaldi (2000). These easily-checkable conditions on the state-space quadruple (A, B, C, D) ensure that all associated state variables and system output remain non-negative at every time instant for every non-negative initial state and every non-negative input.

Externally positive systems, on the other hand, map monotonically increasing inputs to monotonically increasing outputs, a property known to be satisfied for a single-input, single-output (SISO) LTI system if and only if its impulse response is non-negative. Despite this simply-stated definition, the complete characterization of external positivity remains stubbornly elusive (Farina and Rinaldi, 2000, p. 11); see also Drummond et al. (2019).

Zemanian (1960) established several sufficient conditions for a continuous-time, LTI SISO system to exhibit a monotone nondecreasing step response, equivalent to a non-negative impulse response (NNIR) and hence external positivity. Numerous authors have subsequently presented a range of sufficient conditions for NNIR in terms of pole-zero patterns; see for example Liu and Bauer (2008); Drummond et al. (2019) and the references therein.

Grussler and Rantzer (2014) presented a tractable, state-space-based sufficiency test for external positivity, verification of which for a given rational transfer function is known to be NP-hard; see Bell et al. (2010). The sufficiency test in Grussler and Sepulchre (2019) employs an impulse response product of Ebihara (2018) to derive a state-space characterization of external positivity, but the Kronecker

product in (Grussler and Sepulchre, 2019, Theorem 1) implies that this characterization does not necessarily encompass all low-order systems, e.g. third-order systems.

Of key importance to the present paper is the work of Lin and Fang (1997), in which necessary and sufficient conditions are presented for a third-order SISO LTI system to have a monotone nondecreasing step response; see also Jiang et al. (2001). For third-order systems having real poles, a comprehensive characterization of external positivity is therefore presented in Theorem 5 of Lin and Fang (1997). The characterization is nonetheless very complicated, and does not extend to the case of systems having complex poles.

In this paper, we exploit the equivalence between the impulse response of an externally positive system having unity DC gain with a probability density function (pdf) of a continuous random variable, and hence equate the associated cumulative distribution function (cdf) with the unit step response. In this way, we are able to leverage a rich literature from stochastic modeling (specifically, so-called matrix-exponential distributions; Bean et al. (2008)) to simplify the characterization of external positivity of third-order systems in Lin and Fang (1997), and to extend the characterization to the case of complex poles.

In studying fundamental performance limitations for a class of positive nonlinear systems, Goodwin et al. (2018) established an intriguing property exhibited by stable all-pole linear systems, namely that the impulse response $g(t)$ of any such system satisfies the property that $\dot{g}(t)/g(t)$ is a non-increasing function of time $t > 0$; see (Goodwin et al., 2018, Lemma 32). This result invites the following questions: (a) does there exist a physical interpretation of this property? (b) are there linear systems other than all-pole systems for which the property holds? If so, how are they characterized?

An intuitively appealing answer to question (a) comes from very recent work of Grussler and Sepulchre (2019), wherein the notion of *strong unimodality* of a system is defined. Strongly unimodal systems map unimodal inputs (i.e. signals having a unique maximum) to unimodal outputs. It is shown in Grussler and Sepulchre (2019) that an LTI system with impulse response $g(t)$ satisfies the $\dot{g}(t)/g(t)$ non-increasing property if and only if it preserves unimodality from input to output, i.e. is strongly unimodal.

In this paper, we address question (b) for strictly proper third-order systems expressed in transfer function form. For this class of systems, we present a method for calculating the region in $\mathbb{R}^2$ which—for a user-specified set of three real poles—completely describes the set of numerator coefficients such that the resulting system is strongly unimodal. Central to the proposed method is the fact that strong unimodality of a given third-order system is equivalent to external positivity of an appropriately defined auxiliary system which is itself third-order.

Pharmacokinetics is a branch of pharmacology that studies drug concentrations in various organs and tissue groups as a function of time and dose. Since drug concentrations are necessarily non-negative, and since drug concentrations are often simply assumed to monotonically decline after discontinuation of bolus (pulse-like) drug administration, pharmacokinetics is a very natural domain for the application of the concepts of external positivity and strong unimodality; see Chellaboina et al. (2004). We illustrate the application of the results in this paper to a third-order pharmacokinetic model for the absorption, distribution, metabolism and excretion of remifentanil, an ultra-short acting opioid analgesic often used during general anaesthesia; see Cascone et al. (2013).

The remainder of this paper is organized as follows. Section 2 establishes notation, and summarizes key background results on monotone nondecreasing step response, matrix exponential distributions and strong unimodality. Section 3 presents a method for calculating the region of strong unimodality for a third-order system with prescribed real poles. In Section 4 the results of the two previous sections are applied in a pharmacokinetic setting. Concluding remarks and directions for future research are presented in Section 5.

2. PRELIMINARIES

2.1 Notation

The set of nonnegative real numbers is denoted by $\mathbb{R}_{\geq 0} := \{x \in \mathbb{R} : x \geq 0\}$, and the set of all nonnegative functions is denoted by $\mathcal{S}_{\geq 0} := \{g : \mathbb{R} \to \mathbb{R}_{\geq 0}\}$.

For a real-valued function $g : \mathbb{R} \to \mathbb{R} \cup \{-\infty\}$, we say that it is *concave* if $g(\lambda x + (1-\lambda)y) \geq \lambda g(x) + (1-\lambda)g(y)$ for all $0 \leq \lambda \leq 1$. The set of all concave functions is denoted by $\mathcal{S}_{\mathrm{c}}$. The set of all integrable functions is denoted by L_1. The *convolution* of two real-valued functions g and u is defined as $(g * u)(t) = \int_{-\infty}^{\infty} f(t-\tau)g(\tau)d\tau$. For $\mathcal{A} \subset \mathbb{R}$, the *indicator function* is defined as

$$\mathbb{1}_{\mathcal{A}}(x) = \begin{cases} 1 & x \in \mathcal{A}, \\ 0 & x \notin \mathcal{A}. \end{cases}$$

In the sequel, we shall commonly refer to a system via its transfer function, with only a mild abuse of terminology.

2.2 Monotone nondecreasing step response

Consider a third-order linear SISO linear system with a non-strictly proper transfer function

$$G(s) = K\frac{cs^3 + bs^2 + as + 1}{ps^3 + qs^2 + rs + 1}, \tag{1}$$

where the gain $K > 0$ is set to one without loss of generality, and where

$$ps^3 + qs^2 + rs + 1 = (T_1 s + 1)(T_2 s + 1)(T_3 s + 1), \tag{2}$$

with $T_1 \geq T_2 \geq T_3 > 0$.

In this paper, we identify an equivalence between the impulse response of an externally positive system on the one hand, and the probability density function of a non-negative random variable on the other. Alternatively, an equivalence is identified between a monotone nondecreasing step response of a linear system and the cumulative distribution function of a continuous random variable taking only non-negative values.

Theorem 1. (Lin and Fang (1997)). A necessary and sufficient condition for the monotone nondecreasing step re-

sponse of (1)–(2) with three distinct real negative poles, i.e. $T_1 > T_2 > T_3$ is that

$$c \leq bT_1T_2T_3/((T_1T_2 + T_2T_3 + T_3T_1) \tag{3}$$

and

$$T_1^2(a - T_1) - T_1b + c \leq 0, \tag{4a}$$
$$T_2^2(a - T_2) - T_2b + c \geq 0 \tag{4b}$$

and

$$T_2^2(a - T_2) - T_2b + c < 0, \tag{5a}$$
$$[T_2T_3/(T_2 + T_3)]\,(b - T_2T_3) \leq c \tag{5b}$$

and

$$T_1^2(a - T_1) - T_1b + c \leq 0, \tag{6a}$$
$$T_2^2(a - T_2) - T_2b + c < 0, \tag{6b}$$
$$[T_2T_3/(T_2 + T_3)]\,(b - T_2T_3) > c, \tag{6c}$$
$$\frac{T_1(T_2 - T_3)}{T_3(T_1 - T_2)} \ln \frac{T_2^2[T_1^2(a - T_1) - T_1b + c]}{T_1^2[T_2^2(a - T_2) - T_2b + c]} \geq \ln \frac{T_3^2[T_2^2(a - T_2) - T_2b + c]}{T_2^2[T_3^2(a - T_3) - T_3b + c]} < 0. \tag{6d}$$

Proof. See Lin and Fang (1997), noting that proofs of supporting lemmas in the Appendix of Lin and Fang (1997) are omitted due to space limitations; see, however, Horváth et al. (2009); Kolossváry and Telek (2011).

Remark 2. Due to space limitations, Theorem 1 is stated only for the case of three real distinct poles, namely the type A case in Lin and Fang (1997). See Theorem 5 in Lin and Fang (1997) for the case of two or more repeated (real) poles.

2.3 Parameterizing the region Ω_3

In Bean et al. (2008), a region Ω_p is defined which characterizes so-called matrix exponential distributions of order p, defined as probability distributions for which the Laplace transform is a rational function of order p. In explicitly recognising the equivalence between probability density functions and the impulse response of (suitably normalized) linear systems, in this paper we are able to leverage the rich stochastic modeling literature to address a long-standing difficult problem of characterizing external positivity, albeit limited to third-order systems, namely to the region Ω_3. We denote by $\partial\Omega_3$ the boundary of Ω_3.

While the interested reader is referred to Bean et al. (2008) and the referencies therein for details on matrix exponential distributions, it is sufficient for the purposes of the present paper to note that the region Ω_3 precisely and succinctly characterizes those third-order LTI systems for which the impulse response is non-negative.

The boundary $\partial\Omega_3$ is defined in (Bean et al., 2008, Theorem 4.1) via the intersection of an infinite family of half-planes. In this paper we require a representation of $\partial\Omega_3$ as a parametric curve, as follows.

Theorem 3. (Fackrell (2009)). Let

$$G(s) = \frac{a_3s^2 + a_2s + a_1}{s^3 + b_3s^2 + b_2s + b_1}, \tag{7}$$

where a_i, b_i are all real and such that $0 < a_1/b_1 \leq 1$, and suppose that the zeros $-\lambda_1, -\lambda_2$ and $-\lambda_3$, of $b(s) = s^3 + b_3s^2 + b_2s + b_1$, are all real and such that $0 < \lambda_1 < \lambda_2 < \lambda_3$. Define θ_1, θ_2 and θ_3 via

$$\tan\theta_1 = \frac{1}{\lambda_2 + \lambda_3}, \quad \pi < \theta_1 < \frac{3\pi}{2} \tag{8}$$
$$\tan\theta_2 = \frac{\lambda_1}{\lambda_2\lambda_3 + \lambda_1\lambda_2 - \lambda_2\lambda_3}, \quad \pi < \theta_2 < 2\pi, \tag{9}$$
$$\text{and} \quad \tan\theta_3 = \frac{1}{\lambda_2}, \quad 0 < \theta_3 < \frac{\pi}{2}. \tag{10}$$

Then a parametric representation of $\partial\Omega_3$ is as follows:

(1) for $\theta_1 < \theta \leq \theta_2$,
$$x_1(\theta) = -\lambda_1 \cot\theta + \lambda_1(\lambda_2 + \lambda_3), \tag{11a}$$
$$x_2(\theta) = 0. \tag{11b}$$

(2) for $\theta_2 < \theta \leq \theta_3 + 2\pi$,
$$x_1(\theta) = \frac{(\lambda_1^2 + \lambda_2\lambda_3)\cos\theta - \lambda_1^2(\lambda_2 + \lambda_3)\sin\theta}{\cos\theta - \lambda_1\sin\theta}, \tag{12a}$$
$$x_2(\theta) = \frac{\lambda_1\cos\theta + (\lambda_2\lambda_3 - \lambda_1\lambda_3 - \lambda_1\lambda_2)\sin\theta}{\cos\theta - \lambda_1\sin\theta}. \tag{12b}$$

(3) for $\theta_3 < \theta \leq \theta_1$,
$$x_1(\theta) = \frac{\lambda_1(\lambda_3 - \lambda_1)(\lambda_2 - \lambda_1)\cos\theta}{L(\theta)} + \lambda_1(\lambda_2 + \lambda_3), \tag{13a}$$
$$x_2(\theta) = \frac{\lambda_1(\lambda_3 - \lambda_1)(\lambda_2 - \lambda_1)\sin\theta}{L(\theta)} + \lambda_1 \tag{13b}$$

where
$$L(\theta) = \lambda_1(\cos\theta - \lambda_1\sin\theta) - \lambda_3(\cos\theta - \lambda_3\sin\theta)\cdot\gamma(\theta)^{(\lambda_1-\lambda_3)/(\lambda_3-\lambda_2)}, \tag{14a}$$
$$\gamma(\theta) = \frac{\lambda_3(\cos\theta - \lambda_3\sin\theta)}{\lambda_2(\cos\theta - \lambda_2\sin\theta))}. \tag{14b}$$

In (Bean et al., 2008, Theorem 4.1) it is shown that $\partial\Omega_3$ consists of:

(1) straight line segment between $O := (0, 0)$ and $R := (\lambda_2\lambda_3, 0)$,
(2) straight line segment between R and $S := (\lambda_3(\lambda_2 + \lambda_1), \lambda_3)$, and
(3) parametric curve Σ_3, which has as its endpoints O and S.

Example 4. Consider

$$G(s) = \frac{a_3s^2 + a_2s + 6}{(s + 1)(s + 2)(s + 3)}, \tag{15}$$

wherein $\lambda_i = i$ for $i = 1, 2, 3$. The three line segments comprising $\partial\Omega_3$, parameterized by (11), (12) and (13), are shown in Figure 1, where $x_i := a_{i+1}$ for $i = 1, 2$. The three endpoints of the line segments are $O = (0, 0), R = (6, 0)$ and $S = (9, 3)$. Also shown as a dotted line in Figure 1 is the closed parametric curve Σ_3^* as defined in (13) but for $0 \leq \theta \leq 2\pi$. The curve Σ_3^* plays a key role in §3.2.

Remark 5. The characterization of the boundary $\partial\Omega_3$ in Theorem 3 is far more explicit than Theorem 1, wherein Ω_3 is implicitly defined as the intersection of regions in $\mathbb{R}^2$ which are not necessarily disjoint and not always half-spaces; see (6). Moreover, (Fackrell, 2009, Theorem 6.2) provides a parameterization of $\partial\Omega_3$ when two of the zeros of $b(s)$ are a complex conjugate pair, thereby completing

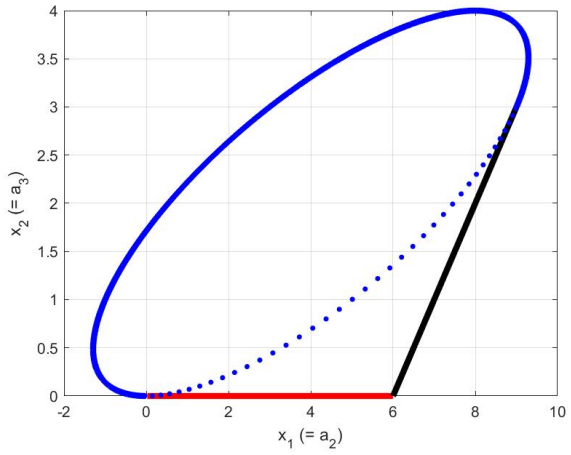

Fig. 1. Boundary $\partial\Omega_3$ for $G(s)$ defined in (15), with line segments (11), (12) and (13) shown in red, black and blue, respectively. Dotted line shows the closed parametric curve Σ_3^* defined in (13) for $0 \le \theta \le 2\pi$

the partial characterization in (Lin and Fang, 1997, Theorem 6), which provides only two necessary conditions for the case of complex poles; see also Jiang et al. (2001).

Remark 6. Theorem 1 can be used to easily check a given point (x_1, x_2) for containment within Ω_3, obviating the need for the more computationally intensive semi-infinite programming approach proposed in Fackrell (2012).

2.4 Strong unimodality

This section collects key results on strong unimodality; the proofs of all results here can be found in Grussler and Sepulchre (2019) and the references therein.

Definition 7. (External positivity). An LTI system with impulse response $g\mathbb{1}_{[0,\infty)}$ is called *externally positive* if

$$\forall u \in \mathcal{S}_{\ge 0} \ : \ g * u \in \mathcal{S}_{\ge 0}$$

Lemma 8. An LTI system is externally positive if and only if its impulse response is nonnegative.

Lemma 9. An LTI system with impulse response g is externally positive if and only if for all monotonically increasing $u \in \mathcal{S}_{\ge 0}$ it holds that $y = g * u \in \mathcal{S}_{\ge 0}$ is monotonically increasing.

Definition 10. (Unimodality). A function $g : \mathbb{R} \to \mathbb{R}$ is called *unimodal* if one the following equivalent conditions hold:

(1) g has a unique maximum, i.e. there exists a mode $m \in \mathbb{R}$ such that f is monotonically increasing on $(-\infty, m]$ and monotonically decreasing on $[m, +\infty)$
(2) g is quasi-concave, i.e.,
$$g(\lambda x + (1-\lambda)y) \ge \min\{g(x), g(y)\}$$
for all x, y and $\lambda \in [0, 1]$.

The set of all unimodal functions is denoted by $\mathcal{S}_{\text{qc}}$.

Definition 11. (Strong unimodality). An LTI system with impulse response g is called *strongly unimodal* if

$$\forall u \in \mathcal{S}_{\text{qc}} : g * u \in \mathcal{S}_{\text{qc}}$$

Lemma 12. A causal LTI system with impulse response $g \in L_1$ is strongly unimodal if and only if $g\mathbb{1}_{[0,\infty)} \in \mathcal{S}_{\ge 0}$ and

$$\dot{g}(t)^2 - g(t)\ddot{g}(t) \ge 0, \qquad \forall t \ge 0. \tag{16}$$

Remark 13. Condition (16) is equivalent to the statement that $\dot{g}(t)/g(t)$ is a non-increasing function of time $t > 0$. See also the appendix of Goodwin et al. (2018), which draws heavily on the notion of log-concavity.

A well-known necessary condition for external positivity is the existence of a dominant, negative-real pole; see Zemanian (1960); Fackrell (2003). If a strongly unimodal system is of order three, then the three poles are necessarily real; see Theorem 2 in Grussler and Sepulchre (2019). Hence the focus on real poles only in the present paper is not especially restrictive. Nonetheless, this leaves to future research the consideration of cases of two or more repeated real poles, and the case of biproper (i.e. proper but not strictly proper) transfer functions $G(s)$.

3. STRONGLY UNIMODAL REGION FOR THIRD-ORDER SYSTEMS

3.1 Region of strong unimodality for third-order systems

The following Lemma is central to the present paper. For third-order systems $G(s)$ it states that the auxiliary system $\tilde{G}(s)$ is itself third-order. Hence to check if a given third-order system is strongly unimodal, we need simply check if the associated (third order) auxiliary system is externally positive.

Lemma 14. Let $g(t) = \gamma_1 e^{-\lambda_1 t} + \gamma_2 e^{-\lambda_2 t} + \gamma_3 e^{-\lambda_3 t}$, and let $G(s) = \mathcal{L}\{g(t)\}$ and $\tilde{G}(s)$ denote the Laplace transform of $g(t)$ and $\tilde{g}(t) := \dot{g}(t)^2 - g(t)\ddot{g}(t)$, respectively. Then

(1)
$$\tilde{g}(t) = \Gamma_{12} e^{-\Lambda_{12} t} + \Gamma_{13} e^{-\Lambda_{13} t} + \Gamma_{23} e^{-\Lambda_{23} t},$$
where
$$\Gamma_{ij} := -\gamma_i \gamma_j (\lambda_i - \lambda_j)^2,$$
$$\Lambda_{ij} := \lambda_i + \lambda_j,$$
for $i, j = 1, 2, 3$ where $i < j$.

(2)
$$\tilde{G}(s) = \frac{\tilde{a}_3 s^2 + \tilde{a}_2 s + \tilde{a}_1}{(s + \Lambda_{12})(s + \Lambda_{13})(s + \Lambda_{23})}$$
where
$$\tilde{a}_1 = \Gamma_{12}\Lambda_{13}\Lambda_{23} + \Gamma_{13}\Lambda_{12}\Lambda_{23} + \Gamma_{23}\Lambda_{12}\Lambda_{13},$$
$$\tilde{a}_2 = \Gamma_{12}(\Lambda_{13}+\Lambda_{23}) + \Gamma_{13}(\Lambda_{12}+\Lambda_{23}) + \Gamma_{23}(\Lambda_{12}+\Lambda_{13}),$$
$$\tilde{a}_3 = \Gamma_{12} + \Gamma_{13} + \Gamma_{23}.$$

Proof.

(1) The result follows on direct substitution of
$$\dot{g}(t) = -\gamma_1\lambda_1 e^{-\lambda_1 t} - \gamma_2\lambda_2 e^{-\lambda_2 t} - \gamma_3\lambda_3 e^{-\lambda_3 t}$$
$$\ddot{g}(t) = \gamma_1\lambda_1^2 e^{-\lambda_1 t} + \gamma_2\lambda_2^2 e^{-\lambda_2 t} + \gamma_3\lambda_3^2 e^{-\lambda_3 t}.$$
into the expression $\dot{g}(t)^2 - g(t)\ddot{g}(t)$, noting cancellations between terms $\gamma_i\lambda_i e^{-2\lambda_i t}$ in $\dot{g}(t)^2$ and $g(t)\ddot{g}(t)$ for $i = 1, 2, 3$.
(2) Follows immediately from properties of Laplace transform.

Example 15. Consider the system

$$G(s) = \frac{0.25s^2 + 3s + 6}{(s+1)(s+2)(s+3)}, \tag{17}$$

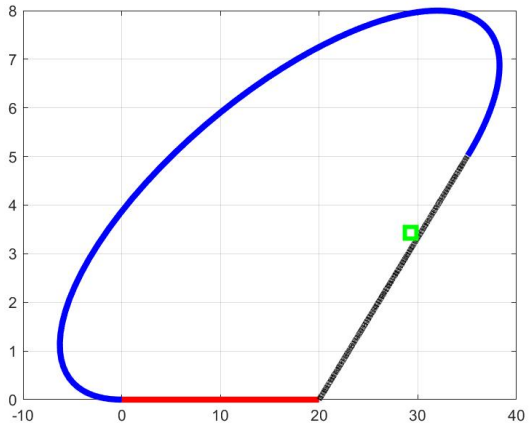

Fig. 2. Boundary $\partial\tilde{\Omega}_3$ for the auxiliary $\tilde{G}(s)$ defined in (18). The point $(29.2740, 3.4269)$ marked via green square lies within the region $\tilde{\Omega}_3$, thus $\tilde{G}(s)$ is externally positive hence $G(s)$ in (17) is strongly unimodal

whose corresponding (a_2, a_3) representation $(3, 0.25) \in \Omega_3$ shown in Figure 1, hence is potentially strongly unimodal i.e. satisfies the necessary condition. To test for strong unimodality, it follows via Lemma 14 that the (unity DC-gain normalized) auxiliary system has transfer function

$$\tilde{G}(s) = \frac{3.4269s^2 + 29.2740s + 60}{(s+3)(s+4)(s+5)}, \tag{18}$$

which, as a third-order system, is amenable to testing for external positivity. See Figure 2, which shows that point $(29.2740, 3.4269)$ lies within the region $\tilde{\Omega}_3$ computed via application of Theorem 3 to the system $G(s)$ defined in (17). It follows that $G(s)$ is indeed strongly unimodal.

Since Ω_3 is a closed and bounded (namely, compact) region, and external positivity is a necessary (but not sufficient) condition for strong unimodality, a means of computing the region $\tilde{\Omega}_3$ is thereby suggested, in which the region Ω_3 is gridded, and each grid point (a_2, a_3) is tested for membership in Ω_3.

Example 16. For the class of systems $G(s)$ defined in (15), Figure 3 shows $\tilde{\Omega}_3$, the region in (a_2, a_3)-space in which $G(s)$ is strongly unimodal. This non-convex region was generated by gridding the compact region Ω_3 shown in Figure 1, and for each grid point $(a_2, a_3) \in \Omega_3$, using the method illustrated in Example 15 to test for external positivity of the associated auxiliary system.

3.2 Region of strong unimodality: a conjecture and a disproof

Based on the general shape of the region $\tilde{\Omega}_3$, it is natural to conjecture as follows:

Conjecture 17. Given a third-order LTI system whose transfer function is given by (7), the upper edge of the region $\tilde{\Omega}_3$ defining the region of strong unimodality for the system is the lower branch of the parameterized curve Σ_3^* defined in (13) for $0 \le \theta \le 2\pi$.

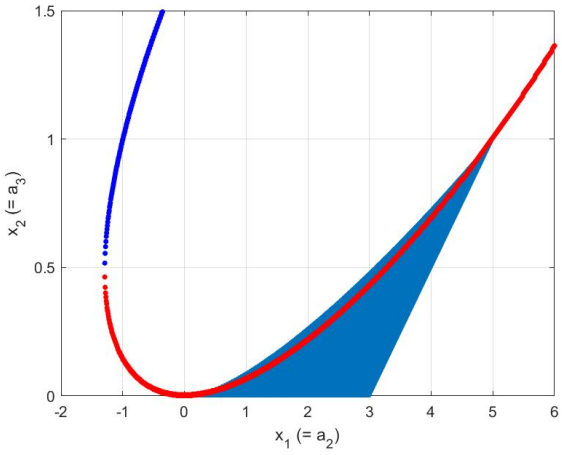

Fig. 3. Non-convex region shaded blue depicts region $\tilde{\Omega}_3$ in (a_2, a_3)-space in which $G(s)$ defined in (15) is strongly unimodal. Also shown is Σ_3^*, with upper and lower branches shown as blue and red lines, respectively

To disprove Conjecture 17, we seek a system which is strongly unimodal, yet whose representation lies strictly above the lower branch of the corresponding parameterized curve Σ_3^*. To this end, consider the system

$$G(s) = \frac{0.48s^2 + 3s + 6}{(s+1)(s+2)(s+3)}, \tag{19}$$

noting that the point $(3, 0.48)$ lies strictly above the corresponding point $(3, 0.4293)$ on the lower branch of Σ_3^*. From a partial fraction expansion of (19), it follows that

$$g(t) = 1.74e^{-t} - 1.92e^{-2t} + 0.66e^{-3t},$$

and thus, via Lemma 14, that

$$\tilde{g}(t) = \dot{g}(t)^2 - g(t)\ddot{g}(t) = 3.3408e^{-3t} - 4.5936e^{-4t} + 1.2672e^{-5t}.$$

Application of Theorem 1 in Horváth et al. (2009) confirms that $\tilde{g}(t) \ge 0$ for all $t \ge 0$. Hence via Lemma 12 it follows that system (19) is strongly unimodal and Conjecture 17 is disproved.

Extensive numerical experiments with a range of randomly-generated systems strongly suggest that the vertices of $\partial\tilde{\Omega}_3$ corresponding to points R and S on $\partial\Omega_3$ are given by $\tilde{R} := (\lambda_1\lambda_3, 0)$ and $\tilde{S} := (\lambda_1(\lambda_2 + \lambda_3), \lambda_1)$. Hence in Figure 3, for example, $\tilde{S} = (3, 0)$ and $\tilde{R} = (5, 1)$.

4. APPLICATION TO PHARMACOKINETICS

4.1 Compartmental models

Pharmacokinetics (PK) is a branch of pharmacology that studies the movement of drugs in the body, starting from administration to Absorption, Distribution, Metabolism and Excretion (ADME). Absorption describes how the drug moves from the site of administration e.g. oral, to blood; distribution describes how the drug is distributed through the various components of the body; metabolism describes how the drug compound breaks down into other compounds (known as metabolites); and excretion describes how the drug and its metabolites are removed from the body; Kurada and Chen (2018); Brunton et al. (2018).

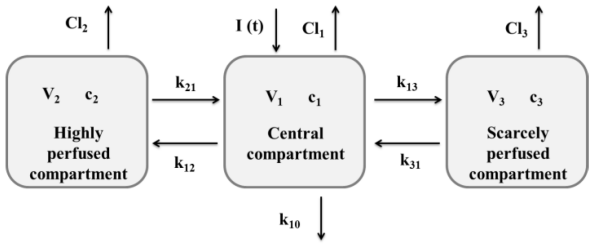

Fig. 4. Three-compartment model from Cascone et al. (2013), where clearance rates Cl_i are herein denoted σ_i

Pharmacokinetics studies drug movement as a function of time and dose; see Brunton et al. (2018); Wagner (1975). By using actual or predicted drug concentrations in various compartments, drug disposition in a patient can be understood. Compartments are not necessarily actual anatomical spaces or physiological volumes, but rather conceptual volumes describing such as blood, organs, fat and lean tissue etc. into which a drug appears to distribute. The behaviour of a drug is assumed kinetically homogeneous within each compartment; see Jacquez and Simon (1993); Anderson (1983); Kajiya et al. (1984).

Compartment models describe the relationship between the drug concentration and time; Kurada and Chen (2018). Compartments are therefore helpful in understanding how a drug moves and distributes within the body, so that when a drug is given to a patient—and its chemistry, also patient mass/height and other attributes are known—the drug kinetics can be predicted; see Rescigno (1960). A large class of PK models are derived on the basis of the compartment concept.

In early phase clinical trials, several doses of a drug are administered to a patient or group of patients, and drug concentrations are subsequently measured at specific times. PK modelling predicts and describes ADME of administered therapies. It requires knowledge of the amount and time of drug administered, route, and enough concentration measurements to describe peak concentrations, half-life and area under a concentration-time curve (known as exposure) for a number of patients. Models can be used to evaluate the effects of disease, age and drug interactions on PK parameters such as volume of distribution, half-life and clearance that require dose alteration.

When multiple samples are difficult or impractical e.g. paediatric setting, simulation experiments can be used to create theoretical PK profiles after a single drug dose, using the range of PK parameters determined from previous patient populations with rich PK sampling. Hundreds of hypothetical patients can then be simulated in order to ascertain an expected range of drug concentrations likely after a dose, for that patient, with individual-specific pharmacokinetics based on patient body mass and height; see Cascone et al. (2018).

It is commonly assumed that as drugs are metabolised and then eliminated, drug concentrations will monotonically decline after discontinuation of drug administration. However, variable distribution of some drugs into specific compartments and subsequently into clearance organs can occur for some drugs. There can also be additional complications of changes in sizes of compartments as well as different capacity of an individuals metabolic and elimination organs to clear drugs. Modelling using compartmental systems can be used to predict drug concentrations which do not decay monotonically (e.g., underdamped oscillations) after discontinuation of drug administration.

4.2 A numerical example

While higher-order, physiologically-based, models are possible (e.g. Levitt and Schnider (2005); Cascone et al. (2018)), by far the most common in clinical practice are 1-, 2- and 3-compartment models. In 3-compartment modeling, the three compartments describe the fate of a drug once administered: the central compartment, which represents the plasma; the highly perfused compartment, representing organs and tissues highly perfused by the blood; and the scarcely perfused compartment, which represents the remaining organs and tissues; see Cascone et al. (2013); Liu et al. (2019).

Consider the following model describing concentrations of the drug remifentanil in three compartments presented in Cascone et al. (2013):

$$V_1\frac{dC_1}{dt} = -\sigma_1 C_1 + k_{21}V_2C_2 + k_{31}C_3V_3 - (k_{12}+k_{13}+k_{10})C_1V_1 + I(t), \tag{20}$$

$$V_2\frac{dC_2}{dt} = k_{12}C_1V_1 - k_{21}C_2V_2 - \sigma_2 C_2, \tag{21}$$

$$V_3\frac{dC_3}{dt} = k_{13}C_1V_1 - k_{31}C_3V_2 - \sigma_3 C_3, \tag{22}$$

in which (20), (21) and (22) are mass balance equations describing the drug concentrations in the central, highly perfused, and scarcely perfused compartments, respectively. Similarly, $V_\star$ denotes the compartment volumes, $\sigma_\star$ are the clearances (rates of drug elimination) from each compartment. The $k_\star$ terms are transport coefficients (or first-order fractional rate constants) between compartments, with k_{10} the kinetic constant of drug elimination from the central compartment. Finally, $I(t)$ in (20) denotes the injection of the drug into the central compartment.

Example 18. Assemble (20)–(22) into a state-space system with state vector $x(t) = [C_1(t), C_2(t), C_3(t)]'$,

$$A = \begin{bmatrix} -(k_{12}+k_{13}+k_{10}) - \dfrac{\sigma_1}{V_1} & k_{21}\dfrac{V_2}{V_1} & k_{31}\dfrac{V_3}{V_1} \\ k_{12}\dfrac{V_1}{V_2} & -k_{21} - \dfrac{\sigma_2}{V_2} & 0 \\ k_{13}\dfrac{V_1}{V_3} & 0 & -k_{31} - \dfrac{\sigma_3}{V_3} \end{bmatrix}, \tag{23}$$

$$B = [1/V_1, 0, 0]', \quad \text{and} \quad C = [1, 0, 0]. \tag{24}$$

Using the parameter values $V_\star, k_\star$ and $\sigma_\star$ in (Cascone et al., 2013, Table I), compute the transfer function $C(sI - A)^{-1}B$ then normalize for unity DC gain to obtain:

$$G(s) = \frac{0.5414s^2 + 0.08431s + 0.001347}{s^3 + 1.001s^2 + 0.09531s + 0.001347}, \tag{25}$$

from which $\lambda_1 = 0.0172, \lambda_2 = 0.0874$ and $\lambda_3 = 0.8968$, i.e. the three poles are real and distinct. The point

$(0.08431, 0.5414)$ is strictly inside the region Ω_3 (not shown) hence the system (25) from drug injection $I(t)$ to the concentration $C_1(t)$ in the central compartment is externally positive, i.e. has a non-negative impulse response. The system (25) is *not* strongly unimodal, however, since application of Theorem 1 in Horváth et al. (2009) confirms that $\dot{g}(t)^2 - g(t)\ddot{g}(t)$ is not non-negative for all $t \geq 0$.

5. CONCLUSION

In this paper, we have shown how an exact, geometric solution to the problem of characterizing external positivity of a third-order linear SISO system is available by drawing on the stochastic modeling literature. The equivalence between the impulse response of an externally positive system on the one hand, and the probability density function of a non-negative random variable on the other, does not appear to have been previously recognised in this context. In particular, the partial characterization of external positivity by Lin and Fang (1997) for third-order systems can be simplified and extended to the case of complex poles by applying the results of Bean et al. (2008). This characterization in turn paves the way for geometrically characterizing the region of strong unimodality for third-order systems with user-specified real poles, since that region is characterized by external positivity of a system which is itself third-order.

While the methods in this paper are limited to third-order systems, they nonetheless find application in pharmacokinetics, in which third-order compartmental systems are in widespread usage. In this setting, strong unimodality is of central clinical relevance, in the sense of establishing whether or not a pulse-like drug infusion necessarily leads to a pulse-like drug concentration profile. Extension of the results to systems having order four and greater remain quite unclear, with only sparse results in the stochastic modeling literature for Ω_p for $p \geq 4$; see (Fackrell, 2003, Chapter 6) and He et al. (2019). The cases of repeated poles, and biproper $G(s)$ i.e. non-zero point mass at zero in the stochastic interpretation, are left to future research, as is the problem of obtaining a closed-form expression for the boundary $\partial\tilde{G}(s)$ of the auxiliary system.

ACKNOWLEDGEMENTS

The first author (SRW) is indebted to Prof. Arie Feuer for articulating the non-increasing property of $\dot{g}(t)/g(t)$ for all-pole systems, and to Prof. Graham Goodwin for his encouragement of the research in this paper over an extended period.

REFERENCES

Anderson, D.H. (1983). *Compartmental Modeling and Tracer Kinetics*, volume 50 of *Lecture Notes in Biomathematics*. Springer-Verlag, Berlin.

Bean, N.G., Fackrell, M., and Taylor, P. (2008). Characterization of matrix-exponential distributions. *Stoch. Models*, 24(3), 339–363.

Bell, P.C., Delvenne, J.C., Jungers, J.M., and Blondel, V.D. (2010). The continuous Skolem-Pisot problem. *Theor. Comput. Sci.*, 411(40–42), 3625–3634.

Brunton, L.L., Hilal-Dandan, R., and Knollmann, B.C. (eds.) (2018). *Goodman & Gilman's: The Pharmacological Basis of Therapeutics*. McGraw-Hill, New York, 13th edition.

Cascone, S., Lamberti, G., Piazza, O., Abbiati, R.A., and Manca, D. (2018). A physiologically-based model to predict individual pharmacokinetics and pharmacodynamics of remifentanil. *Eur. J. Pharm Sci.*, 111, 20–28.

Cascone, S., Lamberti, G., Titomanlio, G., and Piazza, O. (2013). Pharmacokinetics of Remifentanil: A three-compartmental modeling approach. *Transl. Med. UniSa*, 7(4), 18–22.

Chellaboina, V., Haddad, W.M., Bailey, J.M., and Ramakrishnan, R. (2004). On nonoscillation and monotonicity of solutions of nonnegative and compartmental dynamical systems. *IEEE Trans. Biomed. Eng.*, 51(3), 408–414.

Drummond, R., Turner, M.C., and Duncan, S.R. (2019). External positivity of linear systems by weak majorisation. In *Proc. 2019 American Control Conf.*, 5191–5196. Philadelphia, PA, USA.

Ebihara, Y. (2018). H_2 analysis of LTI systems via conversion to externally positive systems. *IEEE Trans. Automat. Control*, 63(8), 2566–2572.

Fackrell, M. (2009). An alternative characterization for matrix exponential distributions. *Adv. Appl. Probab.*, 41(4), 1005–1022.

Fackrell, M. (2012). A semi-infinite programming approach to identifying matrix-exponential distributions. *Int. J. Systems Sci.*, 43(9), 1623–1631.

Fackrell, M.W. (2003). *Characterization of matrix-exponential distributions*. Ph.D. thesis, School of Applied Mathematics, University of Adelaide, Australia.

Farina, L. and Rinaldi, S. (2000). *Positive Linear Systems: Theory and Applications*. John Wiley & Sons, New York.

Goodwin, G.C., Carrasco, D.S., Seron, M.M., and Medioli, A.M. (2018). A fundamental control performance limit for a class of positive nonlinear systems. *Automatica*, 95, 14–22.

Grussler, C. and Rantzer, A. (2014). Modified balanced truncation preserving ellipsoidal cone-invariance. In *Proc. 53rd IEEE Conf. Decision Contr.*, 2365–2370. Los Angeles, CA.

Grussler, C. and Sepulchre, R. (2019). Strongly unimodal systems. In *Proc. 18th Euro. Control Conf. (ECC19)*, 3273–3278. Napoli, Italy.

He, Q.M., Fackrell, M., and Taylor, P. (2019). Characterization of the boundary of the set of matrix-exponential distributions with only real poles. In *Proc. 10th Int. Conf. Matrix-Analytic Methods in Stochastic Models (MAM10)*. Hobart, Australia.

Horváth, A., Rácz, S., and Telek, M. (2009). Moments characterization of order 3 matrix exponential distributions. In K. Al-Begain, D. Fiems, and G. Horváth (eds.), *Analytical and Stochastic Modeling Techniques and Applications (ASMTA 2009), Lecture Notes in Computer Science vol. 5513*, 174–188. Springer-Verlag, Berlin Heidelberg.

Jacquez, J.A. and Simon, C.P. (1993). Qualitative theory of compartmental systems. *SIAM Rev.*, 35(1), 43–79.

Jiang, X., Gu, D., Huang, Z., and Chen, T. (2001). On monotone nondecreasing step responses of third-order

SISO linear systems with a pair of complex poles. In *Proc. 2001 American Control Conf.*, 547–541. Arlington, VA.

Kajiya, F., Kodama, S., and Abe, H. (eds.) (1984). *Compartmental Analysis: Medical Applications and Theoretical Background*. Karger, Basel.

Kolossváry, I. and Telek, M. (2011). Explicit evaluation of ME(3) membership. In *Proc. 8th Int. Conf. on Quantitative Evaluation of SysTems (QEST'11)*, 11–12. Aachen, Germany.

Kurada, R.R. and Chen, F. (2018). Fitting compartment models using PROC NLMIXED. Paper SAS1883-2018, `https://bit.ly/2Cds4cT`. [Online; accessed 6-Nov-2019].

Levitt, D.G. and Schnider, T.W. (2005). Human physiologically based pharmacokinetic model for propofol. *BMC Anesthesiol.*, 5. Article 4, 29 pp.

Lin, S.K. and Fang, C.J. (1997). Nonovershooting and monotone nondecreasing step responses of a third-order SISO linear system. *IEEE Trans. Automat. Control*, 42(9), 1299–1303.

Liu, Y. and Bauer, P.H. (2008). Sufficient conditions for non-negative impulse response of arbitrary-order systems. In *Proc. 2008 IEEE Asia Pacific Conf. on Circuits and Systems*, 1410–1413. Macau, China.

Liu, Z., Galettis, P., Broyd, S.J., van Hell, H., Greenwood, L.M., de Krey, P., Steigler, A., Zhu, X., Schneider, J., Solowij, N., and Martin, J.H. (2019). Model-based analysis on systemic availability of coadministered cannabinoids after controlled vaporised administration. *Intern. Med. J.* Accepted to appear, first published 1 July 2019, https://doi.org/10.1111/imj.14415 [Online; accessed 9-May-2020].

Rescigno, A. (1960). Synthesis of a multicompartmented biological model. *Biochim. Biophys. Acta.*, 37(3), 463–468.

Wagner, J.G. (1975). *Fundamentals of Clinical Pharmacokinetics*. Drug Intelligence Pubns, Hamilton, IL.

Zemanian, A.H. (1960). The properties of pole and zero locations for nondecreasing step responses. *Trans. Amer. Inst. Elec. Eng., Part I: Communication and Electronics*, 79(4), 421–426.